2018-0904 IJOI
http://www.ijoi-online.org/

SOIL-STRUCTURE INTERACTION, DAMPING AND HIGHER MODE EFFECTS ON THE RESPONSE OF A MID-STORY-ISOLATED STRUCTURE FOUNDED ON MULTIPLE SOIL LAYERS

Chong-Shien Tsai
Department of Civil Engineering, Feng Chia University, Taiwan, R. O. C.

Yan-Ming Wang
Ph. D. Program for Civil Engineering, Water Resources Engineering, and Infrastructure Planning, Feng Chia University, Taiwan, R. O. C.
Corresponding author: ym.wang@livemail.tw

Hui-Chen Su
Department of Water Resources Engineering and Conservation, Feng Chia University, Taiwan, R. O. C.

Abstract

This paper investigates the effects of soil-structure interaction (SSI), higher modes, and damping on the response of a mid-story-isolated structure founded on multiple soil layers overlying bedrock. Closed-form solutions for the entire system which consists of a shear beam type superstructure, seismic isolator, and multiple soil layers overlying bedrock were obtained, while subjected to ground motion. The proposed formulations simplify the problem in terms of well-known frequency and mechanical impedance ratios that can consider the effects of SSI, higher modes, and damping in the entire system, and be capable of explicitly interpreting the major dynamic behavior of a mid-story-isolated structure interacting with the multiple soil layers overlying bedrock. The SSI effects on the dynamic response of a mid-story-isolated structure

because of multiple soil layers overlying bedrock were extensively investigated through a series of parametric studies and physically explained by derived formulations. In addition, the results of numerical exercises show that higher damping provided by the isolator may provoke higher mode response of the superstructure; that the lower structure below the isolator may have significantly larger deformations compared to those of the upper structure above the isolator; and that isolator displacements may be amplified by the SSI effects while compared to those of mid-story-isolated structures with fixed-base.

Keywords: mid-story isolation; seismic isolation; soil-structure interaction; closed-form solution; higher-mode effects; soil stratum; passive control; damping effects

Introduction

To the best of authors' knowledge, the concept of base isolation was first proposed by Touaillon in 1870, as shown in Figure 1. The concept of mid-story isolation that placed the isolation system on the mid-story rather than the base of a building was first proposed by Kohl in 1915, as shown in Figure 2. These techniques have been robust and implemented worldwide for protecting structures from earthquake damage. Kelly and Konstantinidis (2011) reviewed the history of multilayered, laminated rubber bearings. Tsai (2012a, 2012b, 2015) detailed the history of the development and recent advancements of the rolling and sliding types of seismic isolation systems. In recent years, for increasing the degree of freedom of the architectural design and construction feasibility, the concept of mid-story isolation proposed by Kohl in 1915 has attracted more attention from Murakami et al. (2000), Sueoka et al. (2004), Torunbalci and Ozpalanlar (2008), and Wang et al. (2012, 2013), especially in highly populated areas.

Soil provides flexibility, material damping, and radiation damping to the conventional and base-isolated structures founded on soft soil, which modifies the characteristic and seismic responses of the entire system. In the past, there have been many papers published to extensively examine these factors on the responses of conventional structures (Chopra and Gutierrez, 1974; Veletsos and Meek, 1974; Stamos and Beskos, 1995; Manolis et al., 1995; Song and Wolf, 1996; Manolis et al., 1997; Hatzigeorgiou and Beskos, 2010). Su and

Ahmadi (1989) investigated the performance of different types of base isolators for shear beam structures founded on rigid foundations. Without considering the SSI effects, Todorovska and Trifunac (1989) studied the physical phenomena associated with wave passage under long buildings which were modeled by two-dimensional continuum shear beam structures. Several research papers have been published to evaluate the effects of SSI on the seismic responses of base-isolated buildings (Constantinou and Kneifati, 1988; Novak and Henderson, 1989; Tsai et al., 2004; Spyrakos et al., 2009a, b; Li et al., 2011) and bridges (Chaudhary et al., 2001; Vlassis and Spyrakos, 2001; Spyrakos and Vlassis, 2002; Tongaonkar and Jangid, 2003; Sarrazin et al., 2005; Soneji and Jangis, 2008; Stehmeyer and Rizos, 2008).

For the purpose of investigating the effects of soil-structure interaction (SSI) on a base-isolated structure under vertically propagating S-wave ground motion, Constantinou and Kneifati (1988) added one additional degree of freedom (DOF) for the base isolator to the conventional one-story building system proposed by Veletsos and Meek (1974), which resulted in two DOFs for the base-isolated superstructure, which was founded on a half-space foundation. In their model, they used two frequency-dependent stiffness, one for the horizontal direction and the other for the rotation resulted from the stiffness in the vertical direction, to simulate the foundation overlying a half-space. They concluded that the consideration of SSI effects in the analysis of a base-isolated structure is warranted for wave parameter values of less than 10 and values of less than 15 for the ratio of the natural frequency of a fixed-base structure to that of a base-isolated one.

In recent years, the SSI effects on the seismic responses of base-isolated structures have attracted considerable attention, and several research articles have been published on investigating the SSI effects on the dynamic responses of base-isolated building structures. Novak and Henderson (1989) evaluated the modal properties of base-isolated buildings to conclude that the contribution of SSI effects should be considered when the flexibilities of the base isolators and soil are comparable. Tsai et al. (2004) developed a rigorous nonlinear time domain procedure for the analyses of friction pendulum system (FPS)-isolated structures to explore the SSI effects on the seismic responses of these types of structures. From their study, they concluded that the soil flexibility and radiation damping resulting from the half-space should be considered in the dynamic analyses of base-isolated

structures. Spyrakos and coworkers evaluated the SSI effects on a seismically isolated structure founded on a half-space (2009a) and soil stratum (2009b) by utilizing an equivalent 2 DOFs fixed-base structure that had a structural height equivalent to a single DOF (SDOF) system for the superstructure and another DOF for the base isolator. In their model, they assumed that by neglecting the inertia force in the half-space, massless soil was modeled by frequency-independent stiffness and damping. They concluded through extensive numerical analyses that the SSI effects played a significant role on seismically isolated structures subjected to harmonic ground motion, and that SSI effects are considerable for relatively stiff, squat structures. Li et al. (2011) adopted a similar concept to that developed by Spyrakos et al. (2009a, b) to appraise the SSI effects on the natural frequencies and damping of seismically isolated buildings. They concluded that SSI effects play an important role in lengthening the fundamental period of taller and more slender structures with relatively stiff isolation systems. Tsai et al. (2016) has published a study concerning SSI effects on the responses of base-isolated structures, which the seismic isolation systems were implemented on the base of a structure. In the research works, however, opinions on the role of SSI in the dynamic behavior of base-isolated structures vary, and no decisive conclusions about the SSI effects on seismically isolated structures have been reached in these publications.

There is still a great need to more carefully examine the SSI effects on the dynamic response of a base-isolated structure. Furthermore, there has been little report if any associated with the SSI effects resulting from multiple soil layers on the seismic response of a mid-story-isolated structure.

(Editor's note: The following sections of this article are presented in single column to facilitate easier reading.)

Mid-story-isolated structure founded on multiple soil layers overlying bedrock

This section aims to investigate the dynamic characteristics of a mid- story- isolated structure founded on multiple soil layers overlying bedrock. As shown in Figure 3, the continuum shear beam superstructure with a height h and a mid-story isolation system at a height h_1 is subjected to vertically propagating SH waves. Considering the shear deformation in the x direction, the upper structure that is located above the isolator is governed by the following equation (Kramer, 1996):

$$\frac{\partial^2 u}{\partial z^2} + \frac{\eta_{S2}}{G_{S2}} \frac{\partial^3 u}{\partial^2 z \partial t} = \frac{1}{\beta_{S2}^2} \frac{\partial^2 u}{\partial t^2} \quad (1)$$

while $h_1 \leq z \leq h$

where u, G_{S2}, and β_{S2} are the displacement in the x direction, the shear modulus, and the SH-wave velocity of the upper structure, respectively; and η_{S2} is the parameter for defining the equivalent viscosity in the upper structure.

The relationship of the shear stress, $\tau_{xz}(z,t)$, with the shear strain, $\gamma_{xz}(z,t)$, in the upper structure according to the Kelvin–Voigt model is given by (Kramer, 1996):

$$\tau_{xz}(z,t) = G_{S2}\gamma_{xz}(z,t) + \eta_{S2} \frac{\partial \gamma_{xz}(z,t)}{\partial t} \quad (2)$$

while $h_1 \leq z \leq h$

The governing equation for the lower structure that is located below the isolator is given by:

$$\frac{\partial^2 u}{\partial z^2} + \frac{\eta_{S1}}{G_{S1}} \frac{\partial^3 u}{\partial^2 z \partial t} = \frac{1}{\beta_{S1}^2} \frac{\partial^2 u}{\partial t^2} \quad (3)$$

while $0 \leq z \leq h_1$

where G_{S1}, and β_{S1} are the shear modulus and the SH-wave velocity of the lower structure, respectively; and η_{S1} is the parameter for defining the equivalent viscosity in the lower structure. The relationship of the shear stress and shear strain in the lower structure can be obtained as:

$$\tau_{xz}(z,t) = G_{S1}\gamma_{xz}(z,t) + \eta_{S1} \frac{\partial \gamma_{xz}(z,t)}{\partial t} \quad (4)$$

while $0 \leq z \leq h_1$

The stress-free boundary condition at the top of the upper structure, $z = h$, gives:

$$\tau_{xz}(h,t) = 0 \quad (5)$$

The stress in the isolator, $z = h_1$, is given by:

$$\tau_{xz}(h_1,t) = k_b[u(h_1^+,t) - u(h_1^-,t)] - c_b[\dot{u}(h_1^+,t) - \dot{u}(h_1^-,t)] \quad \text{while } h_1^- \leq z \leq h_1^+ \tag{6}$$

where $\dot{u}$ is the vibration velocity of a particle in a medium; k_b and c_b denote the stiffness and damping coefficient per unit area of the isolator, respectively; and $z = h_1^+$ and $z = h_1^-$ denote the locations at the top and bottom of the isolator, respectively. The nonlinear behavior of the isolation system is well known and possible to be modeled by an equivalent linear model that consists of effective stiffness and equivalent damping ratio to simulate the hysteretic behavior of the isolation system (Kelly and Konstantinidis, 2011). As can be seen in Equation (6), the damping of the isolator is helpful for reducing isolator deformation and for transmitting shear force from the lower structure onto the upper structure.

The stress boundary condition at $z = h_1$ is given by:

$$\tau_{xz}(h_1^+,t) = r_m \tau_{xz}(h_1^-,t) \tag{7}$$

where r_m is the ratio of the shear stress at the top of the isolator to that at the bottom of the isolator.

The governing equation for the n^{th} soil layer with a depth of d_n is:

$$\frac{\partial^2 u}{\partial z^2} + \frac{\eta_n}{G_n}\frac{\partial^3 u}{\partial^2 z \partial t} = \frac{1}{\beta_n^2}\frac{\partial^2 u}{\partial t^2} \quad \text{while } -D_n \leq z \leq -D_{n-1} \tag{8}$$

where G_n, β_n, and η_n represent the shear modulus, SH-wave velocity, and the parameter defined as the equivalent viscosity in the n^{th} soil layer, respectively; and D_n denoting the depth of the n^{th} layer of the soil stratum from the ground surface is given by:

$$D_n = d_1 + d_2 + \cdots + d_n \tag{9}$$

The relationship of the shear stress with the shear strain in the n^{th} soil layer in accordance with the Kelvin–Voigt model is given by (Kramer, 1996):

$$\tau_{xz}(z,t) = G_n\gamma_{xz}(z,t) + \eta_n\frac{\partial\gamma_{xz}(z,t)}{\partial t} \quad \text{while } -D_n \le z \le -D_{n-1} \tag{10}$$

The relationship, based on the balance of the shear force, between the shear stresses at the bottom of the lower structure and at the top of the first soil layer can be obtained as:

$$\tau_{xz}(0^+,t) = r_p\tau_{xz}(0^-,t) \tag{11}$$

where r_p is the ratio of the shear stress at the bottom of the lower structure to that at the top of the first layer of soil strata.

The compatible displacements at the interface of the lower structure and the soil layer yields:

$$u(0^+,t) = u(0^-,t) \tag{12}$$

As shown in Figure 3, if the system is subjected to shear deformations in the x direction under vertically propagated shear wave displacements of $1e^{-i\omega t}$, the boundary condition at the bottom of the soil stratum, $z = -D_N$, is:

$$u(-D_N,t) = 1e^{-i\omega t} \tag{13}$$

where ω is the external excitation frequency and N is the total number of soil layers.

For the steady-state dynamic response, the general solution to Equation (1) is given by:

$$u(z,t) = U(z)e^{-i\omega t} \quad \text{while } h_1 \le z \le h \tag{14}$$

Substituting Equation (14) into Equation (1) yields the general solution to the upper structure:

$$u(z,t) = \left(A_{S2}e^{-ik^*_{S2}z} + B_{S2}e^{ik^*_{S2}z}\right)e^{-i\omega t} \quad \text{while } h_1 \le z \le h \tag{15}$$

where A_{S2} and B_{S2} are unknown coefficients to be determined by boundary conditions; and the complex wave number k^*_{S2} is given by:

$$k_{S2}^{*} = \omega \sqrt{\frac{\rho_{S2}}{G_{S2}^{*}}} = k_{S2}^{a} + ik_{S2}^{b} \tag{16}$$

where $G_{S2}^{*} = G_{S2}(1 + 2i\xi_{S2})$; ρ_{S2} and ξ_{S2} are the mass density and damping ratio of the upper structure, respectively; and

$$k_{S2}^{a} = \left[\frac{\rho_{S2}\,\omega^2}{2G_{S2}(1 + 4\xi_{S2}^2)}\left(\sqrt{1 + 4\xi_{S2}^2} + 1\right)\right]^{\frac{1}{2}} \tag{17}$$

and

$$k_{S2}^{b} = \left[\frac{\rho_{S2}\,\omega^2}{2G_{S2}(1 + 4\xi_{S2}^2)}\left(\sqrt{1 + 4\xi_{S2}^2} - 1\right)\right]^{\frac{1}{2}} \tag{18}$$

The shear strain in the upper structure can be generally obtained, with the aid of Equation (15), as:

$$\gamma_{xz}(z,t) = \frac{\partial u(z,t)}{\partial z} = ik_{S2}^{*}\left(-A_{S2}e^{-ik_{S2}^{*}z} + B_{S2}e^{ik_{S2}^{*}z}\right)e^{-i\omega t} \tag{19}$$

while $h_1 \le z \le h$

With the aid of Equation (2), the shear stress in the upper structure can be generally obtained as:

$$\tau_{xz}(z,t) = (G_{S2} - i\omega\eta_{S2})ik_{S2}^{*}\left(-A_{S2}e^{-ik_{S2}^{*}z} + B_{S2}e^{ik_{S2}^{*}z}\right)e^{-i\omega t} \tag{20}$$

while $h_1 \le z \le h$

Satisfying the boundary condition of Equation (5) results in:

$$A_{S2} = B_{S2}e^{i2k_{S2}^{*}h} \tag{21}$$

The general solution to Equation (3) is given by:

$$u(z,t) = \left(A_{S1}e^{-ik_{S1}^{*}z} + B_{S1}e^{ik_{S1}^{*}z}\right)e^{-i\omega t} \quad \text{while } 0 \le z \le h_1 \tag{22}$$

where A_{S1} and B_{S1} are unknown coefficients to be determined by boundary conditions; and the complex wave number k_{S1}^{*} is given by:

$$k_{S1}^{*} = \omega\sqrt{\frac{\rho_{S1}}{G_{S1}^{*}}} = k_{S1}^{a} + ik_{S1}^{b} \tag{23}$$

where $G_{S1}^{*} = G_{S1}(1 + 2i\xi_{S1})$; ρ_{S1} and ξ_{S1} are the mass density and damping ratio of the lower structure, respectively; and

$$k_{S1}^{a} = \left[\frac{\rho_{S1}\omega^2}{2G_{S1}(1+4\xi_{S1}^2)}\left(\sqrt{1+4\xi_{S1}^2}+1\right)\right]^{\frac{1}{2}} \tag{24}$$

and

$$k_{S1}^{b} = \left[\frac{\rho_{S1}\omega^2}{2G_{S1}(1+4\xi_{S1}^2)}\left(\sqrt{1+4\xi_{S1}^2}-1\right)\right]^{\frac{1}{2}} \tag{25}$$

The shear strain in the lower structure can be generally obtained, with the aid of Equation (22), as:

$$\gamma_{xz}(z,t) = \frac{\partial u(z,t)}{\partial z} = ik_{S1}^{*}\left(-A_{S1}e^{-ik_{S1}^{*}z} + B_{S1}e^{ik_{S1}^{*}z}\right)e^{-i\omega t} \quad \text{while } 0 \le z \le h_1 \tag{26}$$

With the aid of Equation (4), the shear stress in the lower structure can be generally obtained, as

$$\tau_{xz}(z,t) = (G_{S1} - i\omega\eta_{S1})ik_{S1}^{*}\left(-A_{S1}e^{-ik_{S1}^{*}z} + B_{S1}e^{ik_{S1}^{*}z}\right)e^{-i\omega t} \quad \text{while } 0 \le z \le h_1 \tag{27}$$

Satisfying the boundary conditions of Equations (6) and (7) yields

$$\begin{Bmatrix} A_{S1} \\ B_{S1} \end{Bmatrix} = \begin{Bmatrix} T_{S1} \\ T_{S2} \end{Bmatrix} B_{S2} \tag{28}$$

where

$$T_{S1} = \frac{1}{2}\left[\frac{(G_{S2} - i\omega\eta_{S2})k_{S2}^*}{r_m(G_{S1} - i\omega\eta_{S1})k_{S1}^*}\left(e^{i2k_{S2}^*h}e^{-ik_{S2}^*h_1} - e^{ik_{S2}^*h_1}\right)\right.$$
$$+\left(1 - i\frac{(G_{S2} - i\omega\eta_{S2})k_{S2}^*}{k_b(1 - i\omega c_b/k_b)}\right)e^{ik_{S2}^*h_1} \tag{29}$$
$$\left.+\left(1 + i\frac{(G_{S2} - i\omega\eta_{S2})k_{S2}^*}{k_b(1 - i\omega c_b/k_b)}\right)e^{i2k_{S2}^*h}e^{-ik_{S2}^*h_1}\right]e^{ik_{S1}^*h_1}$$

and

$$T_{S2} = \frac{1}{2}\left[\frac{(G_{S2} - i\omega\eta_{S2})k_{S2}^*}{r_m(G_{S1} - i\omega\eta_{S1})k_{S1}^*}\left(-e^{i2k_{S2}^*h}e^{-ik_{S2}^*h_1} + e^{ik_{S2}^*h_1}\right)\right.$$
$$+\left(1 - i\frac{(G_{S2} - i\omega\eta_{S2})k_{S2}^*}{k_b(1 - i\omega c_b/k_b)}\right)e^{ik_{S2}^*h_1} \tag{30}$$
$$\left.+\left(1 + i\frac{(G_{S2} - i\omega\eta_{S2})k_{S2}^*}{k_b(1 - i\omega c_b/k_b)}\right)e^{i2k_{S2}^*h}e^{-ik_{S2}^*h_1}\right]e^{-ik_{S1}^*h_1}$$

For a steady-state response, the general solution to Equation (8) for the n^{th} soil layer is given by

$$u_n(z,t) = U_n(z)e^{-i\omega t} = \left(A_n e^{-ik_n^* z} + B_n e^{ik_n^* z}\right)e^{-i\omega t} \tag{31}$$

while $-D_n \le z \le -D_{n-1}$

where u_n is the displacement in the x direction of the n^{th} soil layer, and the complex wave number is expressed as

$$k_n^* = \omega\sqrt{\frac{\rho_n}{G_n^*}} = k_n^a + ik_n^b \tag{32}$$

where $G_n^* = G_n(1 + 2i\xi_n)$; ρ_n and ξ_n are the mass density and damping ratio in the n^{th} soil layer, respectively; and

$$k_n^a = \left[\frac{\rho_n\omega^2}{2G_n(1 + 4\xi_n^2)}\left(\sqrt{1 + 4\xi_n^2} + 1\right)\right]^{\frac{1}{2}} \tag{33}$$

and

$$k_n^b = \left[\frac{\rho_n \omega^2}{2G_n(1+4\xi_n^2)}\left(\sqrt{1+4\xi_n^2}-1\right)\right]^{\frac{1}{2}} \tag{34}$$

Satisfying the boundary conditions at the interface of the lower structure and the soil strata, which are Equations (11) and (12), one obtains the unknown coefficients A_1 and B_1 as

$$\begin{Bmatrix} A_1 \\ B_1 \end{Bmatrix} = \begin{bmatrix} t_{11} & t_{12} \\ t_{21} & t_{22} \end{bmatrix} \begin{Bmatrix} A_{S1} \\ B_{S2} \end{Bmatrix} = T_{ss} \begin{Bmatrix} A_{S1} \\ B_{S2} \end{Bmatrix} \tag{35}$$

where T_{ss} is a 2x2 matrix; and its elements are given as follows

$$\begin{aligned} t_{11} &= \frac{1}{2}\left[1+\frac{(G_{S1}-i\omega\eta_{S1})k_{S1}^*}{r_p(G_1-i\omega\eta_1)k_1^*}\right] \\ t_{12} &= \frac{1}{2}\left[1-\frac{(G_{S1}-i\omega\eta_{S1})k_{S1}^*}{r_p(G_1-i\omega\eta_1)k_1^*}\right] \\ t_{21} &= t_{12} \text{ and } t_{22} = t_{11} \end{aligned} \tag{36}$$

The boundary condition for the displacement at the interface of the n^{th} and $(n+1)^{th}$ layers of soil strata, an identical stress at the depth of D_n ($z=-D_n$), is given by

$$\begin{aligned} u(-D_n,t) &= \left(A_n e^{ik_n^* D_n} + B_n e^{-ik_n^* D_n}\right)e^{-i\omega t} \\ &= \left(A_{n+1} e^{ik_{n+1}^* D_n} + B_{n+1} e^{-ik_{n+1}^* D_n}\right)e^{-i\omega t} \end{aligned} \tag{37}$$

The boundary condition for the stress at the interface of the n^{th} and $(n+1)^{th}$ layers of soil strata, an identical stress at the depth of D_n, can be obtained as

$$\begin{aligned} \tau_{xz}(-D_n,t) &= (G_n - i\omega\eta_n)ik_n^*\left(-A_n e^{ik_n^* D_n} + B_n e^{-ik_n^* D_n}\right)e^{-i\omega t} \\ &= (G_{n+1} - i\omega\eta_{n+1})ik_{n+1}^*\left(-A_{n+1} e^{ik_{n+1}^* D_n} + B_{n+1} e^{-ik_{n+1}^* D_n}\right)e^{-i\omega t} \end{aligned} \tag{38}$$

By solving Equations (37) and (38), one can obtain

$$A_{n+1} = \frac{1}{2}\left[\left(1 + \frac{(G_n - i\omega\eta_n)k_n^*}{(G_{n+1} - i\omega\eta_{n+1})k_{n+1}^*}\right)e^{ik_n^* D_n} A_n + \left(1 - \frac{(G_n - i\omega\eta_n)k_n^*}{(G_{n+1} - i\omega\eta_{n+1})k_{n+1}^*}\right)e^{-ik_n^* D_n} B_n\right] e^{-ik_{n+1}^* D_n} \quad (39)$$

and

$$B_{n+1} = \frac{1}{2}\left[\left(1 - \frac{(G_n - i\omega\eta_n)k_n^*}{(G_{n+1} - i\omega\eta_{n+1})k_{n+1}^*}\right)e^{ik_n^* D_n} A_n + \left(1 + \frac{(G_n - i\omega\eta_n)k_n^*}{(G_{n+1} - i\omega\eta_{n+1})k_{n+1}^*}\right)e^{-ik_n^* D_n} B_n\right] e^{ik_{n+1}^* D_n} \quad (40)$$

Equations (39) and (40) can be written in matrix form as

$$\begin{Bmatrix} A_{n+1} \\ B_{n+1} \end{Bmatrix} = \begin{bmatrix} s_{11} & s_{12} \\ s_{21} & s_{22} \end{bmatrix} \begin{Bmatrix} A_n \\ B_n \end{Bmatrix} = \boldsymbol{S}_n \begin{Bmatrix} A_n \\ B_n \end{Bmatrix} \quad (41)$$

The element s_{11}^n of the 2x2 matrix $\boldsymbol{S}_n$ can be expressed as

$$s_{11}^n = \frac{1}{2}\left(1 + \frac{(G_n - i\omega\eta_n)k_n^*}{(G_{n+1} - i\omega\eta_{n+1})k_{n+1}^*}\right)e^{ik_n^* D_n} e^{-ik_{n+1}^* D_n} \quad (42)$$

The element s_{12}^n of the matrix $\boldsymbol{S}_n$ is given by

$$s_{12}^n = \frac{1}{2}\left(1 - \frac{(G_n - i\omega\eta_n)k_n^*}{(G_{n+1} - i\omega\eta_{n+1})k_{n+1}^*}\right)e^{-ik_n^* D_n} e^{-ik_{n+1}^* D_n} \quad (43)$$

The element s_{21}^n of the matrix $\boldsymbol{S}_n$ is

$$s_{21}^n = \frac{1}{2}\left(1 - \frac{(G_n - i\omega\eta_n)k_n^*}{(G_{n+1} - i\omega\eta_{n+1})k_{n+1}^*}\right)e^{ik_n^* D_n} e^{ik_{n+1}^* D_n} \quad (44)$$

The element s_{22}^n of the matrix $\boldsymbol{S}_n$ can be obtained as

$$s_{22}^n = \frac{1}{2}\left(1 + \frac{(G_n - i\omega\eta_n)k_n^*}{(G_{n+1} - i\omega\eta_{n+1})k_{n+1}^*}\right)e^{-ik_n^* D_n} e^{ik_{n+1}^* D_n} \quad (45)$$

Satisfying the boundary condition of Equation (13) at bottom of the N^{th} soil layer leads to

$$u(-D_N, t) = \left(A_N e^{ik_N^* D_N} + B_N e^{-ik_N^* D_N}\right)e^{-i\omega t} = 1e^{-i\omega t} \quad (46)$$

Equation (46) can be rewritten in matrix form as

$$\begin{Bmatrix} A_N \\ B_N \end{Bmatrix}^T \begin{Bmatrix} e^{ik_N^* D_N} \\ e^{-ik_N^* D_N} \end{Bmatrix} = 1 \quad (47)$$

One can obtain the following equation from Equation (41):

$$\begin{Bmatrix} A_N \\ B_N \end{Bmatrix} = S_{N-1} S_{N-2} \cdots S_2 S_1 \begin{Bmatrix} A_1 \\ B_1 \end{Bmatrix} = S_{SUM} \begin{Bmatrix} A_1 \\ B_1 \end{Bmatrix} \quad (48)$$

where $S_{SUM} = S_{N-1} S_{N-2} \cdots S_2 S_1$.

Substitution of Equations (35) and (28) into Equation (48) yields

$$\begin{Bmatrix} A_N \\ B_N \end{Bmatrix} = S_{SUM} T_{SS} \begin{Bmatrix} T_{S1} \\ T_{S1} \end{Bmatrix} B_{S2} \quad (49)$$

Substituting Equation (49) into Equation (47) leads to

$$B_{S2} \begin{Bmatrix} T_{S1} \\ T_{S1} \end{Bmatrix}^T (T_{SS})^T (S_{SUM})^T \begin{Bmatrix} e^{ik_N^* D_N} \\ e^{-ik_N^* D_N} \end{Bmatrix} = 1 \quad (50)$$

The unknown coefficient B_{S2} can therefore be obtained as from Equation (50)

$$B_{S2} = \frac{1}{Q} \quad (51)$$

where Q is a scalar and given by

$$Q = \begin{Bmatrix} T_{S1} \\ T_{S1} \end{Bmatrix}^T (T_{SS})^T (S_{SUM})^T \begin{Bmatrix} e^{ik_N^* D_N} \\ e^{-ik_N^* D_N} \end{Bmatrix} \quad (52)$$

where

$$(S_{SUM})^T = (S_1)^T (S_2)^T \cdots (S_{N-2})^T (S_{N-1})^T \quad (53)$$

The total displacement at the top of the upper structure, $u(h,t)$, can be obtained as

$$u(h,t) = \frac{2}{Q} e^{ik_{S_2}^* h} e^{-i\omega t} \quad (54)$$

The maximum total displacement at the top of the upper structure, $u(h)_{max}$, is given by

$$u(h)_{max} = \left| \frac{2}{Q} e^{ik_{S_2}^* h} \right| \quad (55)$$

The total displacement at the top of the isolator, $u(h_1^+,t)$, can be obtained as

$$u(h_1^+,t) = \left(\frac{1}{Q}\right) \left[e^{i\left(2k_{S_2}^* h - k_{S_2}^* h_1\right)} + e^{ik_{S_2}^* h_1} \right] e^{-i\omega t} \quad (56)$$

The maximum total displacement at the top of the isolator, $u(h_1^+)_{max}$, can be expressed as

$$u(h_1^+)_{max} = \left|\left(\frac{1}{Q}\right)\left[e^{i\left(2k_{S_2}^* h - k_{S_2}^* h_1\right)} + e^{ik_{S_2}^* h_1}\right]\right| \quad (57)$$

The total displacement at the bottom of the isolator, $u(h_1^-, t)$, is obtained as

$$u(h_1^-, t) = \left(\frac{1}{Q}\right)\left[T_{S1}e^{-ik_{S_1}^* h_1} + T_{S2}e^{ik_{S_1}^* h_1}\right]e^{-i\omega t} \quad (58)$$

The maximum total displacement at the bottom of the isolator, $u(h_1^-)_{max}$, is

$$u(h_1^-)_{max} = \left|\left(\frac{1}{Q}\right)\left[T_{S1}e^{-ik_{S_1}^* h_1} + T_{S2}e^{ik_{S_1}^* h_1}\right]\right| \quad (59)$$

The relative displacement between the top and the bottom of the isolator, $\Delta u(h_1, t)$, which is the deformation of the isolator, can be expressed as

$$\Delta u(h_1, t) = \left(\frac{1}{Q}\right)\left[e^{i\left(2k_{S_2}^* h - k_{S_2}^* h_1\right)} + e^{ik_{S_2}^* h_1} - T_{S1}e^{-ik_{S_1}^* h_1} - T_{S2}e^{ik_{S_1}^* h_1}\right]e^{-i\omega t} \quad (60)$$

The maximum relative displacement between the top and the bottom of the isolator, $\Delta u(h_1)_{max}$, can be expressed as

$$\Delta u(h_1)_{max} = \left|\left(\frac{1}{Q}\right)\left[e^{i\left(2k_{S_2}^* h - k_{S_2}^* h_1\right)} + e^{ik_{S_2}^* h_1} - T_{S1}e^{-ik_{S_1}^* h_1} - T_{S2}e^{ik_{S_1}^* h_1}\right]\right| \quad (61)$$

The relative displacement between the top and the bottom of the upper structure, $\Delta u(h, t)$, can be obtained as

$$\Delta u(h, t) = \left(\frac{1}{Q}\right)\left[2e^{ik_{S_2}^* h} - e^{i\left(2k_{S_2}^* h - k_{S_2}^* h_1\right)} - e^{ik_{S_2}^* h_1}\right]e^{-i\omega t} \quad (62)$$

The maximum relative displacement between the top and the bottom of the upper structure, $\Delta u(h)_{max}$, can be obtained as

$$\Delta u(h)_{max} = \left|\left(\frac{1}{Q}\right)\left[2e^{ik_{S_2}^* h} - e^{i\left(2k_{S_2}^* h - k_{S_2}^* h_1\right)} - e^{ik_{S_2}^* h_1}\right]\right| \quad (63)$$

The relative displacement between the top and the bottom of the lower structure, $\Delta u(h_L, t)$, which is the deformation of the lower structure, can be obtained as

$$\Delta u(h_L, t) = \left(\frac{1}{Q}\right)\left[\left(e^{-ik_{S_1}^* h_1} - 1\right)T_{S1} + \left(e^{ik_{S_1}^* h_1} - 1\right)T_{S2}\right]e^{-i\omega t} \quad (64)$$

The maximum relative displacement between the top and the bottom of the lower structure, $\Delta u(h_L)_{max}$, can be obtained as

$$\Delta u(h_L)_{max} = \left|\left(\frac{1}{Q}\right)\left[\left(e^{-ik_{S_1}^* h_1} - 1\right)T_{S1} + \left(e^{ik_{S_1}^* h_1} - 1\right)T_{S2}\right]\right| \tag{65}$$

The total displacement at the ground surface, $u(0,t)$, is given by

$$u(0,t) = \left(\frac{1}{Q}\right)(T_{S1} + T_{S2})e^{-i\omega t} \tag{66}$$

The maximum total displacement at the ground surface, $u(0)_{max}$, is obtained as

$$u(0)_{max} = \left|\left(\frac{1}{Q}\right)(T_{S1} + T_{S2})\right| \tag{67}$$

The transmissibility of the total displacement at the top of the upper structure with respect to the total displacement at the ground surface, $TR_{TD}(h)$, which is independent of the soil property, is obtained as

$$TR_{TD}(h) = \frac{u(h)_{max}}{u(0)_{max}} = \left|\left(\frac{2}{V}\right)\left(e^{ik_{S_2}^* h}\right)\right| \tag{68}$$

where the variable V is given by

$$V = T_{S1} + T_{S2} \tag{69}$$

The transmissibility of the relative displacement between the top and the bottom of the isolator with respect to the total displacement at the ground surface, $TR_{RD}(h_1)$, can be obtained as

$$\begin{aligned} TR_{RD}(h_1) &= \frac{\Delta u(h_1)_{max}}{u(0)_{max}} \\ &= \left|\left(\frac{1}{V}\right)\left[e^{i\left(2k_{S_2}^* h - k_{S_2}^* h_1\right)} + e^{ik_{S_2}^* h_1} - T_{S1}e^{-ik_{S_1}^* h_1} - T_{S2}e^{ik_{S_1}^* h_1}\right]\right| \end{aligned} \tag{70}$$

The transmissibility of the relative displacement between the top and the bottom of the upper structure with respect to the total displacement at the ground surface, $TR_{RD}(h)$, can be obtained as

$$TR_{RD}(h) = \frac{\Delta u(h)_{max}}{u(0)_{max}} = \left|\left(\frac{1}{V}\right)\left[2e^{ik_{S_2}^* h} - e^{i\left(2k_{S_2}^* h - k_{S_2}^* h_1\right)} - e^{ik_{S_2}^* h_1}\right]\right| \tag{71}$$

From equations derived above, it is assumed that the superstructure is a continuum shear beam structure. Two approaches can be adopted to simulate a real structure by using an equivalent shear beam structure. The first approach is to obtain the equivalent shear wave velocity by assuming that the column of the superstructure deforms in bending only and that

the continuum shear beam deforms in shear only [22, 23]. Another approach is to choose the equivalent natural frequency of the shear beam structure equal to that of the real structure. The latter approach is adopted to more conveniently and explicitly interpret the interactive characteristics of the mid-story-isolated structure and its foundation. The fundamental natural circular frequency for the traditional fixed-base structure, ω_{S2}, is (Das, 1983)

$$\omega_{S2} = \frac{\pi \beta_{S2}}{2h} \tag{72}$$

The fundamental natural circular frequency for the soil stratum with a depth of D_n (fixed-free boundary condition), ω_n, is (Das, 1983)

$$\omega_n = \frac{\pi \beta_n}{2D_n} \tag{73}$$

here, β_n and D_n are the shear-wave velocity and the depth of the n^{th} layer of soil stratum, respectively.

If the superstructure is rigid, the natural circular frequency for the base-isolated structure, ω_b, is:

$$\omega_b = \sqrt{\frac{k_b}{\rho_{S2} h}} \tag{74}$$

The following parameters, with the aid of Equations (72)-(74), are very useful for identifying the characteristics of the entire system:

$$\frac{Z_{S2}\omega}{k_b} = \frac{2}{\pi}\left(\frac{\omega_{S2}}{\omega_b}\right)\left(\frac{\omega}{\omega_b}\right) = \frac{2}{\pi} r_{S2b} r \tag{75}$$

In addition,

$$\frac{\omega h}{\beta_{S2}} = \frac{\pi}{2}\left(\frac{\omega}{\omega_{S2}}\right) = \frac{\pi}{2}\left(\frac{\omega}{\omega_b}\right)\left(\frac{\omega_b}{\omega_{S2}}\right) = \frac{2}{\pi}\frac{r}{r_{S2b}} \tag{76}$$

and

$$\frac{\omega D_n}{\beta_n} = \frac{\pi}{2}\left(\frac{\omega}{\omega_n}\right) = \frac{\pi}{2}\left(\frac{\omega}{\omega_b}\right)\left(\frac{\omega_b}{\omega_n}\right) = \frac{2}{\pi}\frac{r}{r_{fbn}} \tag{77}$$

Also

$$\frac{\omega c_b}{k_b} = 2\xi_b\left(\frac{\omega}{\omega_b}\right) = 2\xi_b r \tag{78}$$

where the parameters of the frequency ratios are defined as

$$r = \frac{\omega}{\omega_b}\ ,\ r_{S2b} = \frac{\omega_{S_2}}{\omega_b}\ ,\ r_{S1b} = \frac{\omega_{S_1}}{\omega_b}\ ,\ r_{fbn} = \frac{\omega_n}{\omega_b}\ ,$$

$$k_{S2}^* h = \frac{\pi}{2}\frac{r}{r_{S2b}}(a_{S2} + ib_{S2})\ ,\ k_{S1}^* h_1 = \frac{\pi}{2}\frac{r}{r_{S1b}}(a_{S1} + ib_{S1})\ ,$$

and $k_{S2}^* h_1 = \frac{\pi}{2}\frac{r}{r_{S2b}}(a_{S2} + ib_{S2})\frac{h_1}{h}$

Using the parameters of Equations (72)-(78) derived above and Equation (55), one can obtain the maximum total roof displacement of the upper structure, $u(h)_{max}$, as

$$u(h)_{max} = \left|\frac{2}{Q}e^{i\frac{\pi}{2}\frac{r}{r_{S2b}}(a_{S_2}+ib_{S_2})}\right| \tag{79}$$

The maximum total displacement at the bottom of the upper structure, $u(h_1^+)_{max}$ of Equation (57), can be expressed as

$$u(h_1^+)_{max} = \left|\left(\frac{1}{Q}\right)\left[e^{i\left(\pi\frac{r}{r_{S2b}}(a_{S_2}+ib_{S_2})-\frac{\pi}{2}\frac{r}{r_{S2b}}(a_{S_2}+ib_{S_2})\frac{h_1}{h}\right)} + e^{i\frac{\pi}{2}\frac{r}{r_{S1b}}(a_{S_1}+ib_{S_1})}\right]\right| \tag{80}$$

The maximum total displacement at the bottom of the isolator, $u(h_1^-)_{max}$ of Equation (59), can be expressed as

$$u(h_1^-)_{max} = \left|\left(\frac{1}{Q}\right)\left[T_{S1}e^{-i\frac{\pi}{2}\frac{r}{r_{S1b}}(a_{S_1}+ib_{S_1})} + T_{S2}e^{i\frac{\pi}{2}\frac{r}{r_{S1b}}(a_{S_1}+ib_{S_1})}\right]\right| \tag{81}$$

The maximum relative displacement between the top and the bottom of the isolator (isolator deformation), $\Delta u(h_1)_{max}$ of Equation (61), can be expressed as

$$\begin{aligned}\Delta u(h_1)_{max} = \left|\left(\frac{1}{Q}\right)\left[e^{i\left(\pi\frac{r}{r_{S2b}}(a_{S_2}+ib_{S_2})-\frac{\pi}{2}\frac{r}{r_{S2b}}(a_{S_2}+ib_{S_2})\frac{h_1}{h}\right)} + e^{i\frac{\pi}{2}\frac{r}{r_{S2b}}(a_{S_2}+ib_{S_2})\frac{h_1}{h}}\right.\right.\\ \left.\left. - T_{S1}e^{-i\frac{\pi}{2}\frac{r}{r_{S1b}}(a_{S_1}+ib_{S_1})} - T_{S2}e^{i\frac{\pi}{2}\frac{r}{r_{S1b}}(a_{S_1}+ib_{S_1})}\right]\right|\end{aligned} \tag{82}$$

The maximum relative displacement between the top and the bottom of the upper structure, $\Delta u(h)_{max}$ of Equation (63), can be expressed as

$$\Delta u(h)_{max} = \left|\left(\frac{1}{Q}\right)\left[2e^{i\frac{\pi}{2}\frac{r}{r_{S2b}}(a_{S2}+ib_{S2})} - e^{i\left(\pi\frac{r}{r_{S2b}}(a_{S2}+ib_{S2})-\frac{\pi}{2}\frac{r}{r_{S2b}}(a_{S2}+ib_{S2})\frac{h_1}{h}\right)}\right.\right.$$
$$\left.\left. - e^{i\frac{\pi}{2}\frac{r}{r_{S2b}}(a_{S2}+ib_{S2})\frac{h_1}{h}}\right]\right| \quad (83)$$

The transmissibility of the relative displacement between the top and the bottom of the isolator, $TR_{RD}(h_1)$ of Equation (70), can be expressed as

$$TR_{RD}(h_1) = \frac{\Delta u(h_1)_{max}}{u(0)_{max}}$$
$$= \left|\left(\frac{1}{V}\right)\left[e^{i\left(\pi\frac{r}{r_{S2b}}(a_{S2}+ib_{S2})-\frac{\pi}{2}\frac{r}{r_{S2b}}(a_{S2}+ib_{S2})\frac{h_1}{h}\right)} + e^{i\frac{\pi}{2}\frac{r}{r_{S2b}}(a_{S2}+ib_{S2})\frac{h_1}{h}}\right.\right. \quad (84)$$
$$\left.\left. - T_{S1}e^{-i\frac{\pi}{2}\frac{r}{r_{S1b}}(a_{S1}+ib_{S1})} - T_{S2}e^{i\frac{\pi}{2}\frac{r}{r_{S1b}}(a_{S1}+ib_{S1})}\right]\right|$$

The transmissibility of the total displacement at the top of the upper structure with respect to the total displacement at the ground surface, $TR_{TD}(h)$ of Equation (68), can be expressed as

$$TR_{TD}(h) = \frac{u(h)_{max}}{u(0)_{max}} = \left|\left(\frac{2}{V}\right)\left(e^{i\frac{\pi}{2}\frac{r}{r_{S2b}}(a_{S2}+ib_{S2})}\right)\right| \quad (85)$$

Parametric Studies and Discussion

(Editor's Note: see all Figures at the end of this article.)

Figures 4-7 show the roof displacement, relative displacement between the top and the bottom of the upper structure, relative displacement between the top and the bottom of the lower structure, and isolator deformation, respectively, under various damping ratios of the isolator when the mid- story-isolated structure is founded on a rigid foundation (without soil) with $r_{S2b} = 4$, $h_1/h = 0.05$ and $\xi_{S2} = \xi_{S1} = 5\%$. It should be noted that hereafter, the abscissa represents the frequency ratio r. It is revealed from these figures that damping is helpful in reducing the structural displacement and deformation (relative displacement) of the first mode but not for higher modes and that damping always helps for the reduction of isolator deformation. Note that the response of the first mode of an isolated structure is always considered to be eliminated in virtue of vibration isolation technology. It is therefore, from the reduction of structural deformation viewpoint, not preferable to comprise high damping in a mi-story isolation system. It is observed that higher mode responses play an important role in the response of a mid-story isolated structure, especially for structural deformation.

For a relatively harder soil condition ($I_s = 0.5$) compared to the structure, Figures 8-11 demonstrate the total the roof displacement, relative displacement

between the top and the bottom of the upper structure, relative displacement between the top and the bottom of the lower structure, and isolator deformation, respectively, with various damping ratios provided by the isolator when the mid-story-isolated structure is founded on one layer of soil with $r_{fb} = 2.5$. The responses of the whole system are larger than those for the case of the mid- story-isolated structure founded on a rigid foundation. It is illustrated that the soil layer plays a role of amplifier to enlarge the response of the entire system by comparing them with Figures 4-7, especially for the third mode response that is the second mode for both structure and soil. As shown in Figures 9 and 10, a higher damping ratio is very helpful in reducing the responses of the first and second (the first mode for the soil layer) modes but not in weakening the responses of higher modes. On the other hand, as shown in Figure 11, higher damping ratios are always useful in decreasing isolator deformation, and the isolator deformation is significantly greater than that of the rigid foundation case, as shown in Figure 7. This means that the design of the displacement capacity of the isolator should consider the SSI effects.

Figures 12-15 demonstrate the roof displacement, relative displacement between the top and the bottom of the upper structure, relative displacement between the top and the bottom of the lower structure, and isolator deformation, respectively, with various damping ratios provided by the isolator when the isolated structure is founded on two layers of soil under the condition of Case 2-1 listed in Table 1 (this case represents one harder soil layer overlying another softer soil layer). As shown in Figures 12-14, a higher damping ratio is very beneficial in reducing the responses of the first and second modes but not in lessening the responses of higher modes. If we can design an isolator to make the first and second natural periods of the entire system long enough, we may be able to eliminate the total responses of the first and second modes by the low energy contained in the long period regime of earthquakes and to minimize the response of the entire system. Note that in this case, only to eliminate the first mode response does not seem to be an optimum way, because the natural frequency of the second mode is very close to that of the first mode. The deformation of the upper structure, however, does not benefit from higher damping ratios provided by the isolator, which transmit the energy onto the upper structure, because its response will be dominated by higher modes. On the other hand, as shown in Figure 15, higher damping ratios are always useful in decreasing isolator deformation, as predicted in Equation (6). The relative displacements between the bottom and the top of the upper and lower structures under various damping ratios, as shown in Figures 13 and 14, are also evidence that a higher damping ratio will induce more deformation in the superstructure if it already eliminates the contribution of the first- and second-mode responses by lengthening the natural period of the entire system through mid-story isolation technology.

For the case of a hard soil layer on another even harder soil layer in soil strata, referring to Case 2-2 as listed in Table 1, Figures 16-19 display the roof displacement, relative displacement between the top and the bottom of the upper structure, relative displacement be-

tween the top and the bottom of the lower structure, and isolator deformation, respectively, with various damping ratios from the isolator. As shown in Figures 17 and 18, the responses of higher modes of the structural deformation are amplified by the first softer soil layer, compared to the second layer, which in turn amplifies the higher mode responses of the superstructure even as it is reduced by the base isolator. The isolator deformation, as shown in Figure 19, increases because the movements of the isolated upper structure and the lower structure might not be in phase. Isolator deformation is always lessened by the isolator damping. This soil condition results in a greater structural deformation than that in Case 2-1 because more vibration energy can transmit onto the superstructure from the interface of the first and second soil layers.

Conclusions

To investigate the SSI effects on the dynamic response of a mid- story- isolated structure founded on multiple soil layers overlying bedrock, closed-form solutions have been obtained and then discussed for various conditions. We can draw the following conclusions after a series of numerical exercises and observations by the derived closed solutions:

(1) The SSI significantly affects the seismic response of a mid-story-isolated structure founded on soil layers overlying bedrock.
(2) Damping of the soil layers and isolator plays both the roles of absorbing and transmitting energy to the upper structure.
(3) The first and second modes of the entire system are governed by the properties of the superstructure and isolator, and a higher damping ratio is, in general, beneficial for reducing the responses of these two modes.
(4) The efficiency of the isolator in reflecting vibrational energy trying to transmit onto the superstructure has no relation with the properties of the soil layers, but it depends on the properties of the superstructure and the isolator.
(5) The higher-mode responses of the entire system are usually dominated by the properties of the soil stratum, and the reduction of the higher-mode responses of the superstructure is generally not benefited by higher damping of the isolator.
(6) The reduction of the response of the structural deformation benefits from the large values of r_{Sb} to reflect energy at the interface of the superstructure and the isolator, even though the motion on the ground surface is amplified because of the large amount of energy reflected from both the superstructure-isolator interface and the bedrock to cause large displacements of the ground surface as well as the large deformation of the isolator.
(7) The SSI effects on the design of the isolator displacement capacity should be considered cautiously because the response of the soil medium might be amplified by the reflected waves from the boundary and the movements of the isolated superstructure and the ground surface might be out of phase.
(8) Higher damping ratios provided by the isolator are generally beneficial for reducing isolator deformation.

References

Chaudhary MTA, Abe M, and Fujino Y (2001), "Identification of Soil-structure Interaction Effect in Isolated Bridges from Earthquake Records," *Soil Dynamics and Earthquake Engineering*, 21(8), pp. 713-725.

Chopra A K and Gutierrez JA (1974), "Earthquake Response Analysis of Multistory Buildings Including Foundation Interaction," *Earthquake Engineering and Structural Dynamics*, 3(1), pp. 65-77.

Constantinou MC and Kneifati MC (1988), "Dynamics of Soil-Base-Isolated-Structure System," *Journal of Structural Engineering, ASCE*, 114(1), pp. 211-221.

Das BM (1983), "Fundamentals of Soil Dynamics," Baker & Taylor Books.

Hatzigeorgiou GD and Beskos DE (2010), "Soil–structure Interaction Effects on Seismic Inelastic Analysis of 3-D Tunnels," *Soil Dynamics and Earthquake Engineering*, 30, pp. 851-861.

Kelly JM and Konstantinidis DA (2011), "Mechanics of Rubber Bearings for Seismic and Vibration Isolation," John Wiley & Sons, Ltd.

Kohl L (1915), "Device for buildings against earthquakes," US Patent No. 1158932.

Kramer SL (1996), "Geotechnical Earthquake Engineering," Prentice-Hall.

Li C, Liu W, Wang S, and Du D (2011), "Analyses of Soil-structure Interaction (SSI) Effects on Seismic Response of Base-isolated Structures," *Advanced Materials Research*, Vols. 163-167: 4199-4207.

Manolis GD, Nikolaou A, and Gazetas G (1997), "Soil-pile-bridge Seismic Interaction: Kinematic and Inertial Effects, Part I: Soft Soil," *Earthquake Engineering and Structural Dynamics*, 26, pp. 337-359.

Manolis GD, Tetepoulidis PI, Talaslidis DG, and Apostolidis G (1995), "Seismic Analysis of Buried Pipeline in A 3D Soil Continuum," *Engineering Analysis with Boundary Elements*, 15, pp. 371–394.

Murakami K, Kitamura H, Ozaki H, and Teramoto T (2000), "Design and Analysis of A Building with the Middle-story Isolation Structural System," *The 12th World Conference on Earthquake Engineering*, Auckland, New Zealand, Paper No. 0857.

Novak M and Henderson P (1989), "Base-isolated Buildings with Soil-structure Interaction," *Earthquake Engineering and Structural Dynamics*, 18, pp. 751-765.

Sarrazin M, Moroni O, and Roesset JM (2005), "Evaluation of Dynamic Response Characteristics of Seismically Isolated Bridges in Chile," *Earthquake Engineering and Structural Dynamic*, 34, pp. 425-448.

Soneji BB and Jangid RS (2008), "Influence of Soil–structure Interac-

tion on the Response of Seismically Isolated Cable-stayed Bridge," *Soil Dynamics and Earthquake Engineering*, 28, pp. 245-257.

Song CH and Wolf JP (1996), "Consistent Infinitesimal Finite-Element Cell Method: Three-dimensional Vector Wave Equation," *International Journal for Numerical Methods in Engineering*, 39, pp. 2189–2208.

Spyrakos CC and Vlassis AG (2002), "Effect of Soil-structure Interaction on Seismically Isolated Bridges," *Journal of Earthquake Engineering*, 6(3), pp. 391-429.

Spyrakos CC, Koutromanos IA, and Maniatakis CA (2009a), "Seismic Response of Base-isolated Buildings Including Soil-structure Interaction," *Soil Dynamics and Earthquake Engineering*, 29, pp. 658-668.

Spyrakos CC, Maniatakis CA, and Koutromanos IA (2009b), "Soil-structure Interaction Effects on Base-isolated Buildings Founded on Soil Stratum," *Engineering Structure*, 31, pp. 729-737.

Stamos AA and Beskos DE (1995), "Dynamic Analysis of Large 3-D Underground Structures by the BEM," *Earthquake Engineering and Structural Dynamics*, 4, pp. 17–34.

Stehmeyer EH and Rizos D (2008), "Considering Dynamic Soil Structure Interaction (SSI) Effects on Seismic Isolation Retrofit Efficiency and the Importance of Natural Frequency Ratio," *Soil Dynamics and Earthquake Engineering*, 28, pp. 468-479.

Su L, Ahmadi G, and Tadjbakhsh IG (1989), "A Comparative Study of Performance of Various Base Isolation Systems, Part I: Shear Beam Structures," *Earthquake Engineering and Structural Dynamics*, 18(11), pp. 11-32.

Sueoka T, Torii S, and Tsuneki Y (2004), "The Application of Response Control Design Using Middle-story Isolation System to High-rise Building," *The 13th World Conference on Earthquake Engineering*, Vancouver, B. C. Canada, Paper No. 3457.

Todorovska MI and Trifunac MD (1989), "Antiplane Earthquake Waves in Long Structures," *Journal of Engineering Mechanics, ASCE*, 115(12), pp. 2687-2708.

Tongaonkar NP and Jangid RS (2003), "Seismic Response of Isolated Bridges with Soil-structure Interaction," *Soil Dynamics and Earthquake Engineering*, 23, pp. 287-302.

Torunbalci N and Ozpalanlar G (2008), "Earthquake Response Analysis of Mid-story Buildings Isolated with Various Isolation Techniques," *The 13th World Conference on Earthquake Engineering*, Beijing, China.

Touaillon J (1870), "Improvement in Buildings," US Letters Patent No. 99973.

Tsai CS (2012a), "Advanced Base Isolation Systems for Light Weight Equipments," Chapter 4 in Earthquake-Resistant Structures - Design, Assessment and Rehabilitation, Edited by Abbas Moustafa, InTech, Croatia.

Tsai CS (2012b), "Recent Advances in Seismic Isolation Systems," *The Fifth Kwang-Hua Forum on Innovations and Implementations in Earthquake Engineering Research*, December 8-10, Shanghai, China.

Tsai CS (2015) "Seismic Isolation Devices: History and Recent Developments," *The ASME 2015 PVP Conference*, July 19-23, 2015, Boston, Massachusetts, USA, Paper No. PVP2015-45068.

Tsai CS, Chen CS, and Chen BJ (2004), "Effects of Unbounded Media on Seismic Responses of FPS-isolated Structures," *Structural Control and Health Monitoring*, 11, pp. 1-11.

Veletsos AS and Meek JW (1974), "Dynamic Behavior of Building-Foundation System," *Earthquake Engineering and Structural Dynamics*, 3, pp. 121-138.

Vlassis AG and Spyrakos CC (2001), "Seismically Isolated Bridge Piers on Shallow Soil Stratum with Soil-structure Interaction," *Computers and Structures*, 79, pp. 2847-2861.

Wang SJ, Chang KC, Hwang JS, Hsiao JY, Lee BH, and Hung YC (2012), "Dynamic Behavior of A Building Structure Tested with Base and Mid-story Isolation Systems," *Engineering Structures*, 42, pp. 420-433.

Wang SJ, Hwang JS, Chang KC, Lin MH, and Lee BH (2013), "Analytical and Experimental Studies on Mid-story Isolated Buildings with Modal Coupling Effect," *Earthquake Engineering and Structural Dynamics*, 42, pp. 201-219.

Table 1. Properties of a mid-story-isolated structure built on two soil layers overlying bedrock

Cases	r_{Sb}	r_{fb1}	r_{fb2}	I_S	$\xi_S\%$	$\xi_1\%$	$\xi_2\%$	β_1/β_2
2-1	4.0	2.5	0.833	0.5	5	2	2	1.5
2-2	4.0	2.5	2.5	0.5	5	2	2	0.5

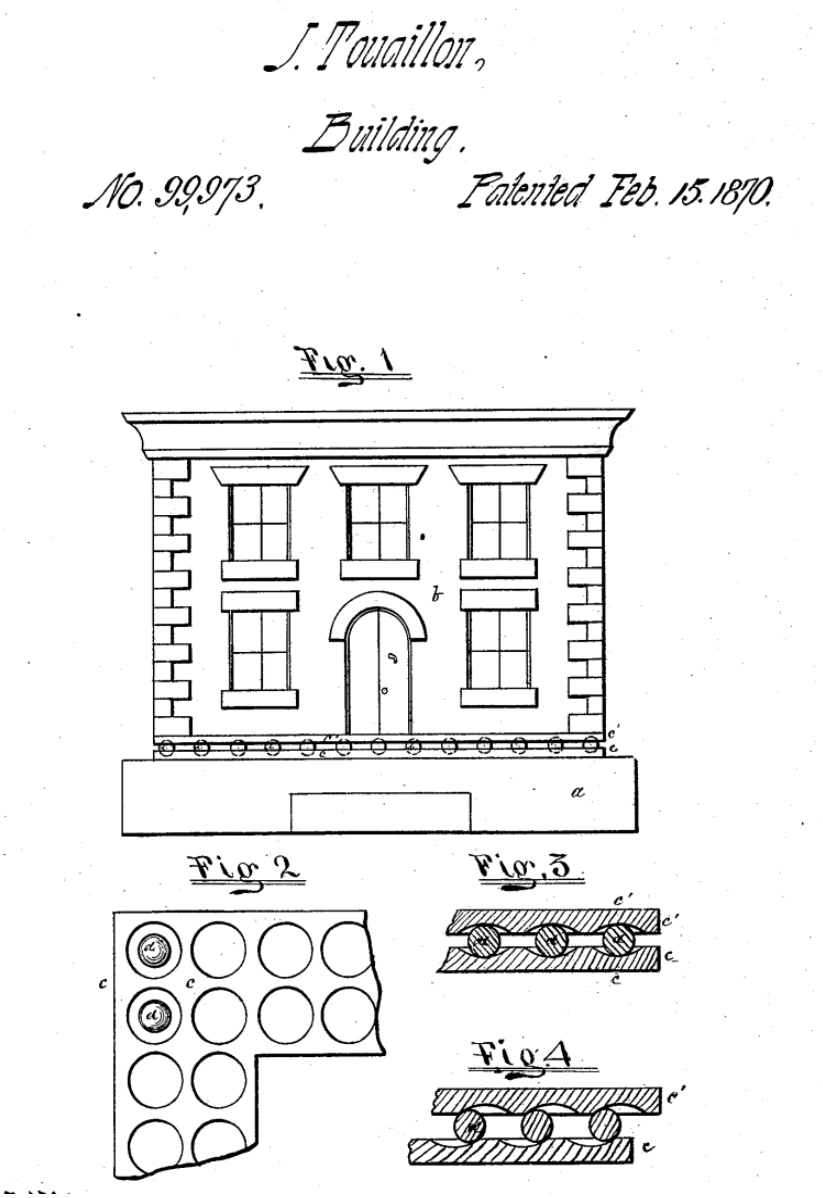

Figure 1. Touaillon's original patent (1870)

L. KOHL.
DEVICE FOR PROTECTING BUILDINGS AGAINST EARTHQUAKES.
APPLICATION FILED JULY 3, 1914.

1,158,932. Patented Nov. 2, 1915.

Fig 1

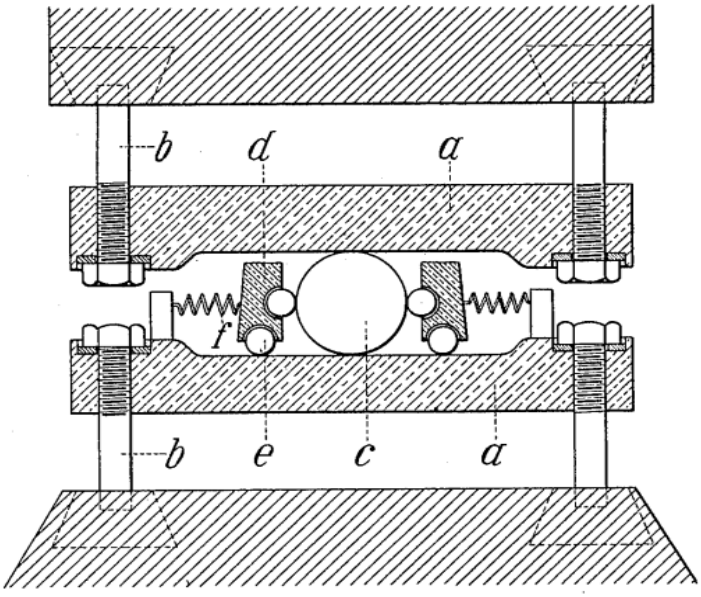

Fig 2

Figure 2. Kohl's original patent (1915)

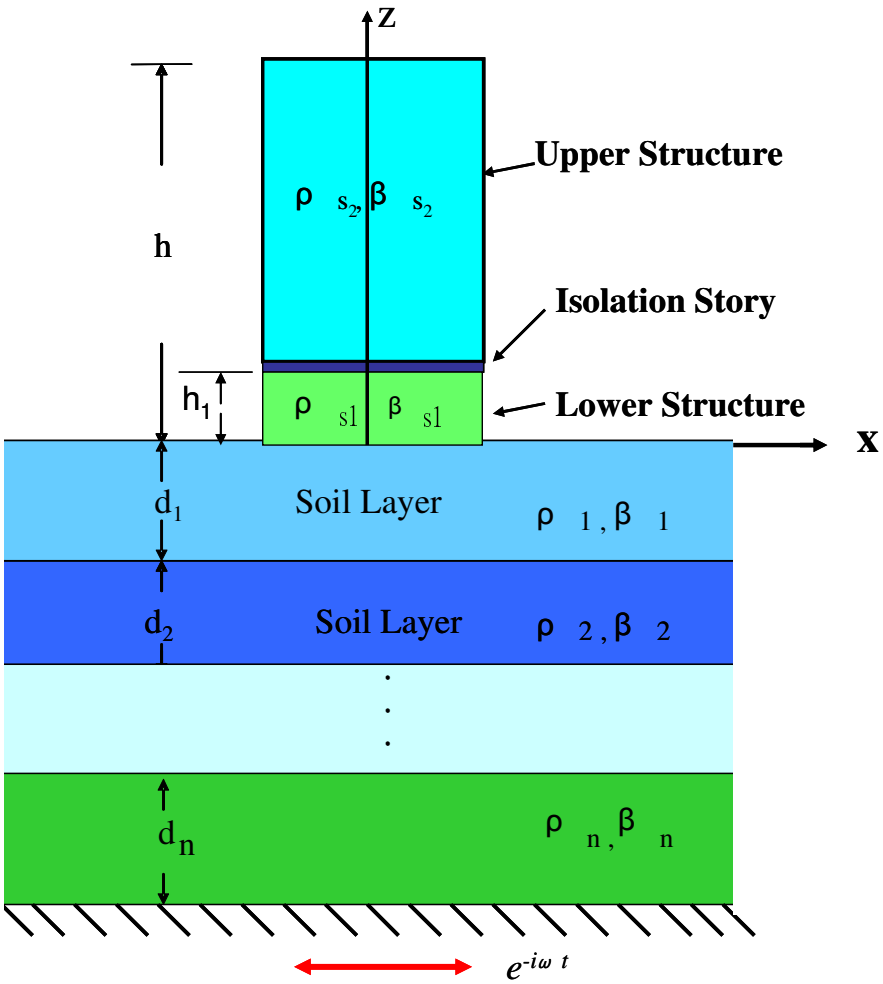

Figure 3. A mid-story-isolated structure founded on soil layers overlying bedrock

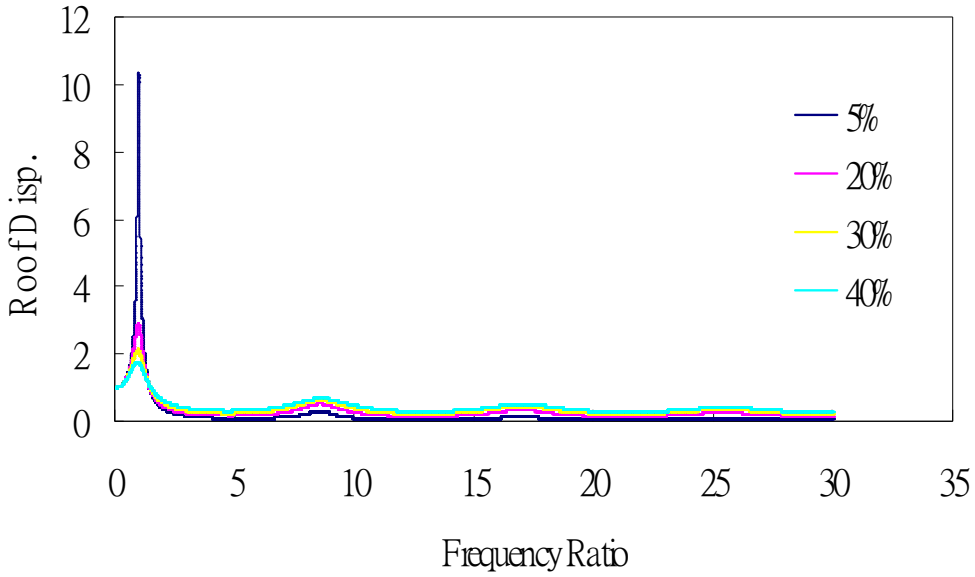

Figure 4. Roof displacement for case of rigid foundation under various damping ratio of isolator

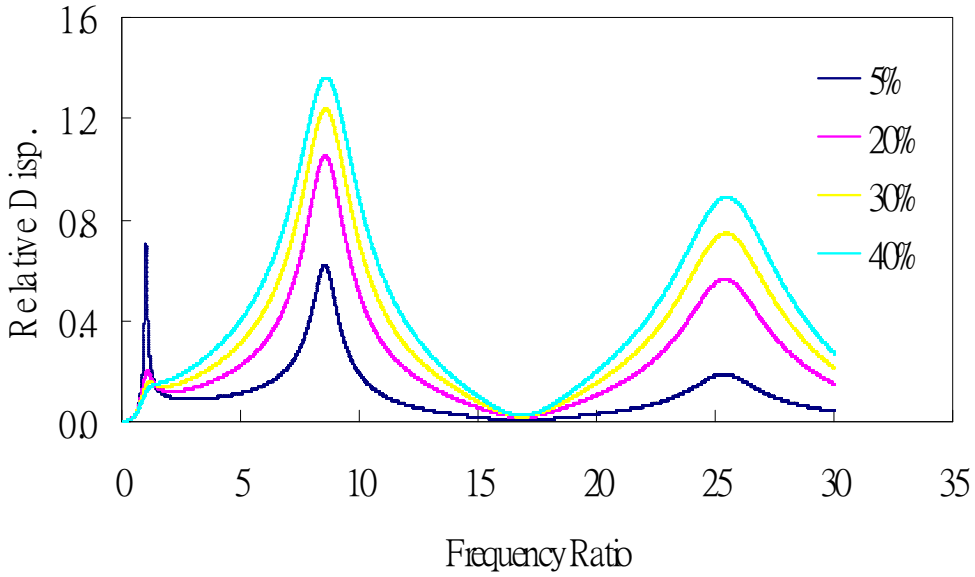

Figure 5. Relative displacement between top and bottom of the upper structure for case of rigid foundation under various damping ratio of isolator

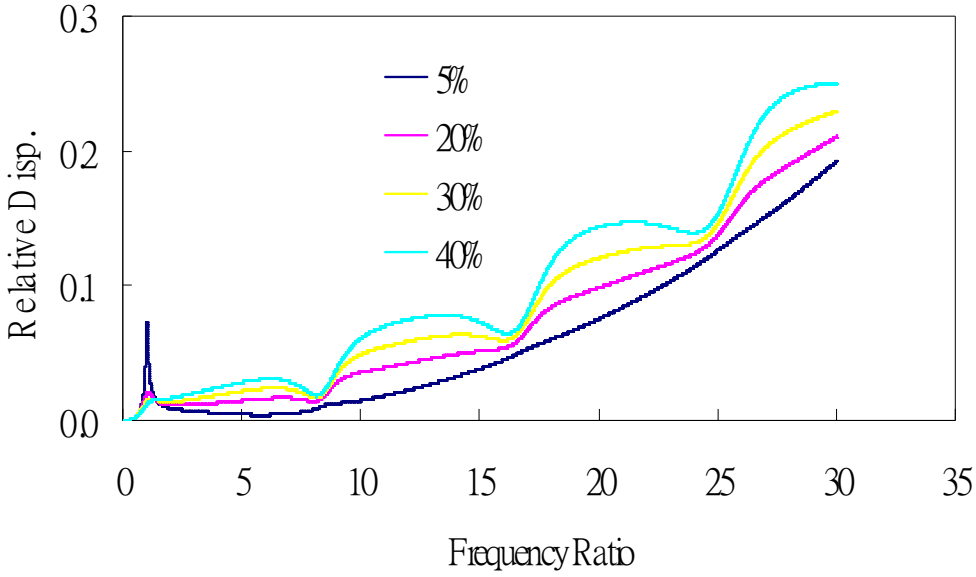

Figure 6. Relative displacement between top and bottom of the lower structure for case of rigid foundation under various damping ratio of isolator

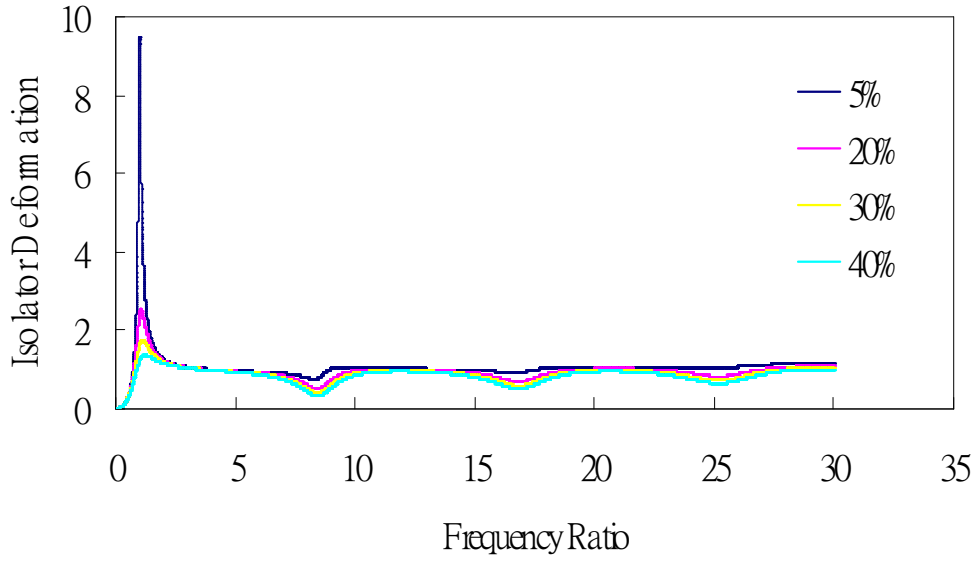

Figure 7. Isolator Deformation for case of rigid foundation under various damping ratio of isolator

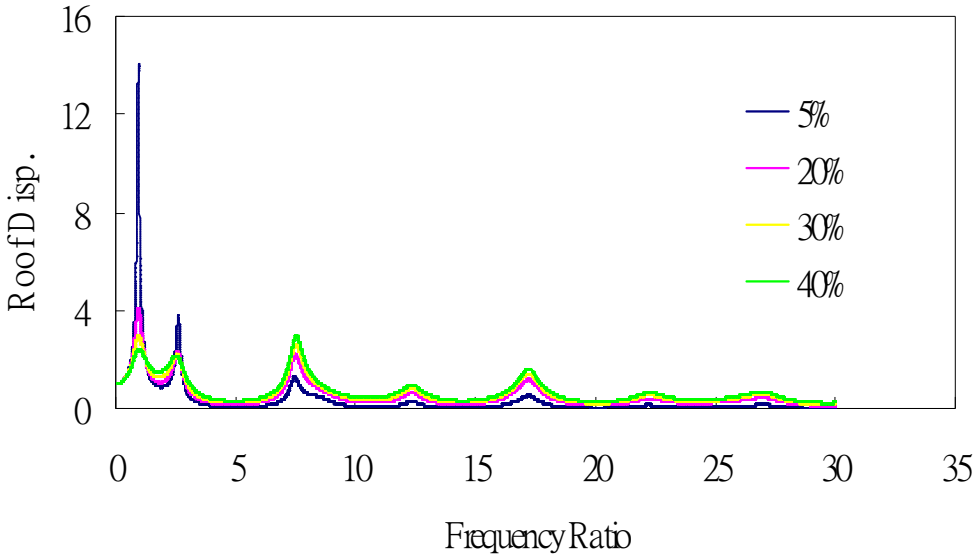

Figure 8. Roof displacement for case of one layer soil under various damping ratio of isolator

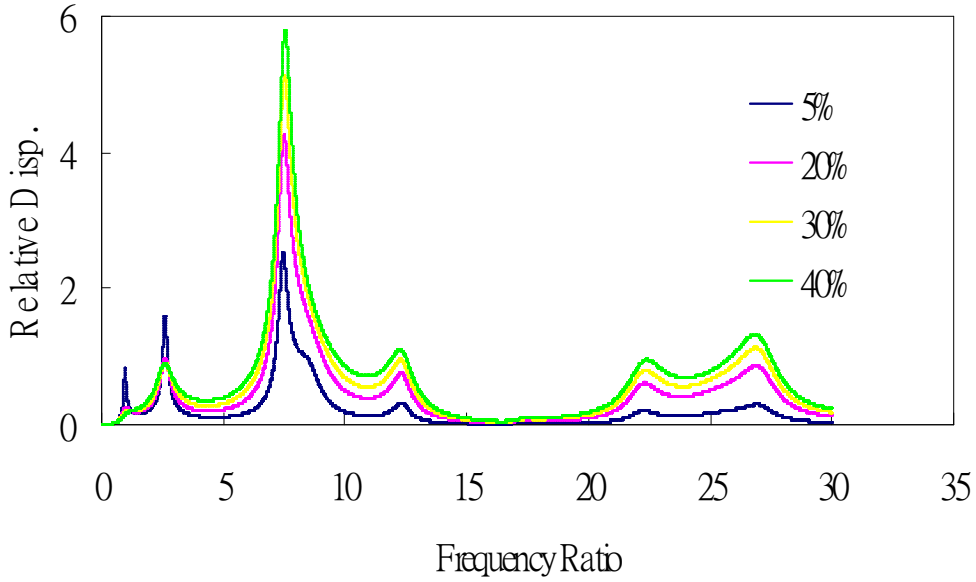

Figure 9. Relative displacement between top and bottom of upper structure for case of one layer soil under various damping ratio of isolator

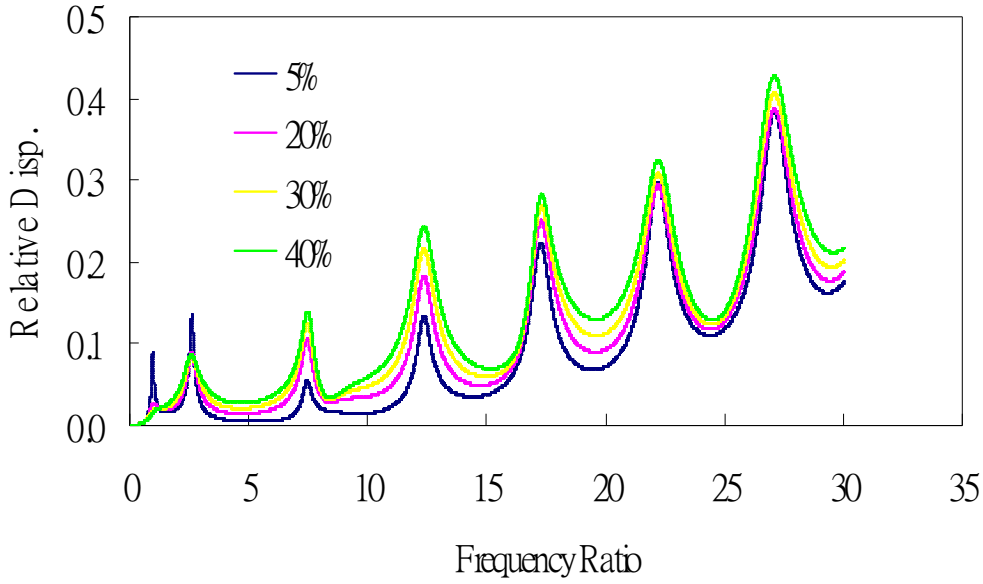

Figure 10. Relative displacement between top and bottom of lower structure for case of one layer soil under various damping ratio of isolator

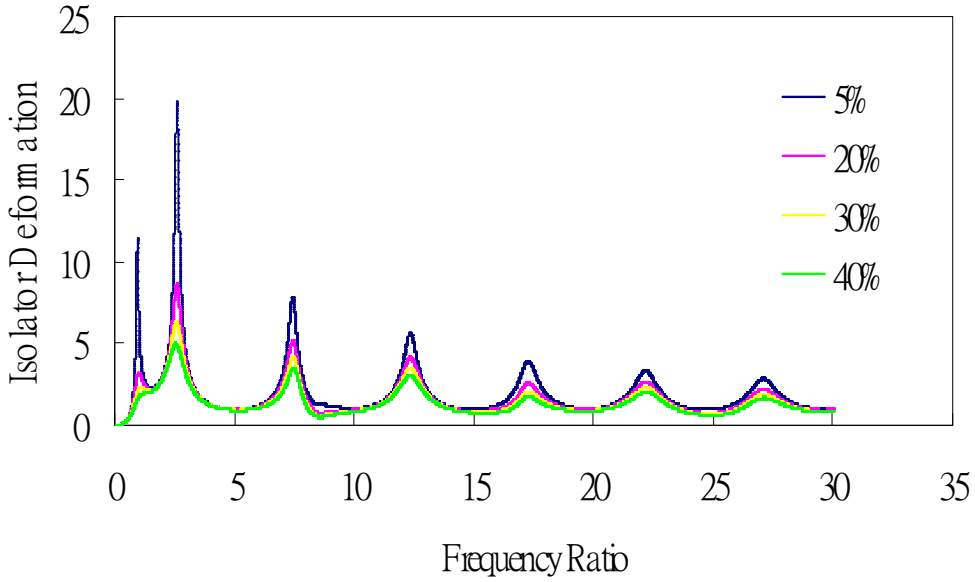

Figure 11. Isolator deformation for case of one layer soil under various damping ratio of isolator

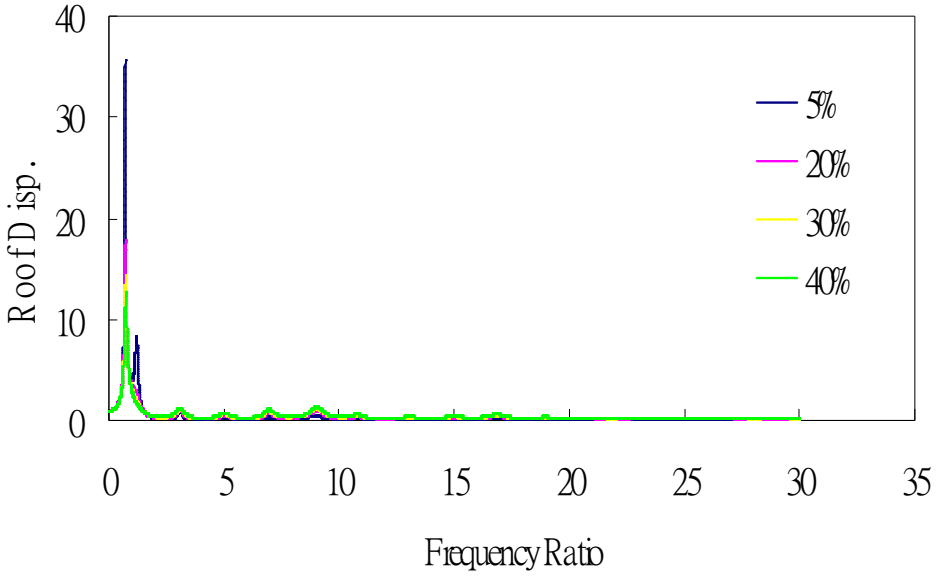

Figure 12. Roof displacement for Case 2-1 under various damping ratio of isolator

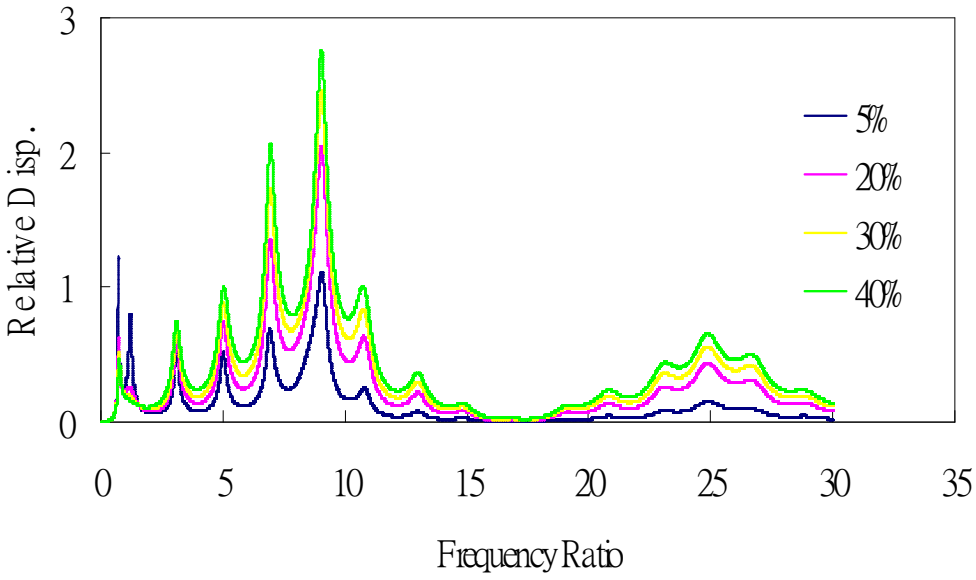

Figure 13. Relative displacement between top and bottom of upper structure for Case 2-1 under various damping ratio of isolator

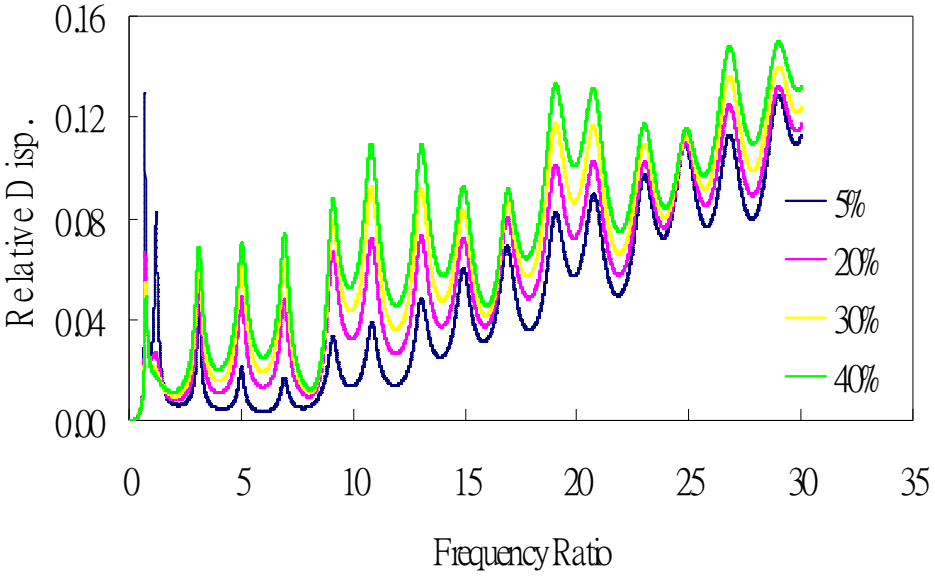

Figure 14. Relative displacement between top and bottom of lower structure for Case 2-1 under various damping ratio of isolator

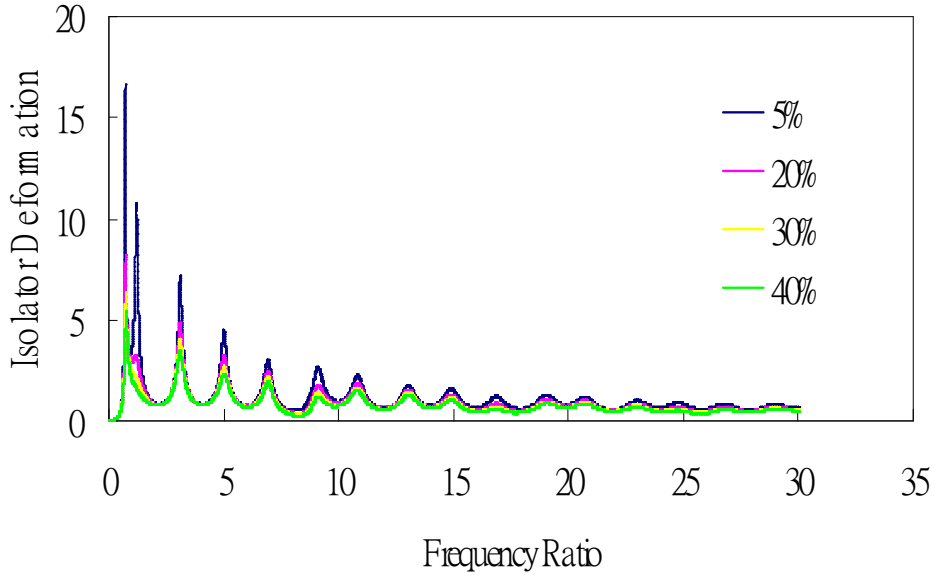

Figure 15. Isolator deformation for Case 2-1 under various damping ratio of isolator

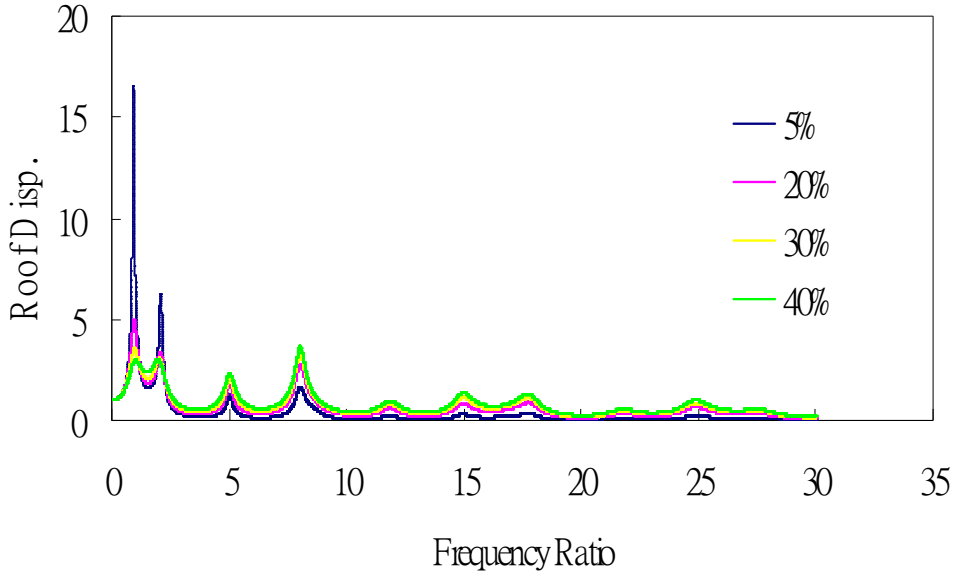

Figure 16. Roof displacement for Case 2-2 under various damping ratio of isolator

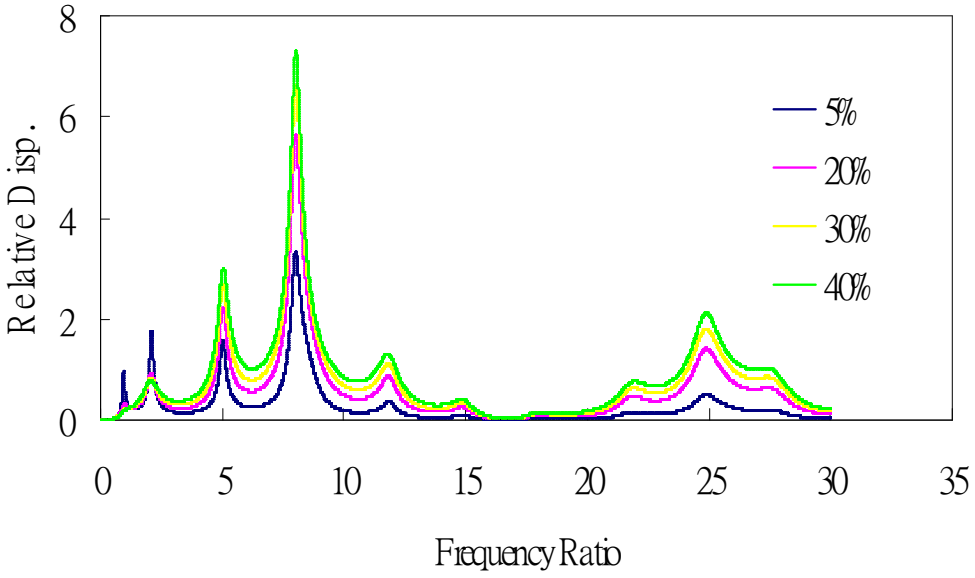

Figure 17. Relative displacement between top and bottom of upper structure for Case 2-2under various damping ratio of isolator

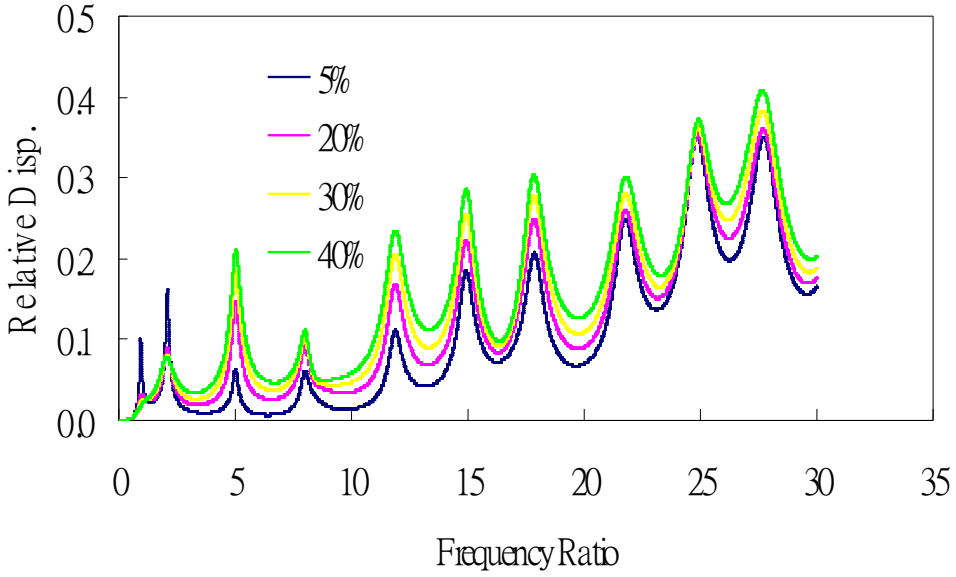

Figure 18. Relative displacement between top and bottom of lower structure for Case 2-2 under various damping ratio of isolator

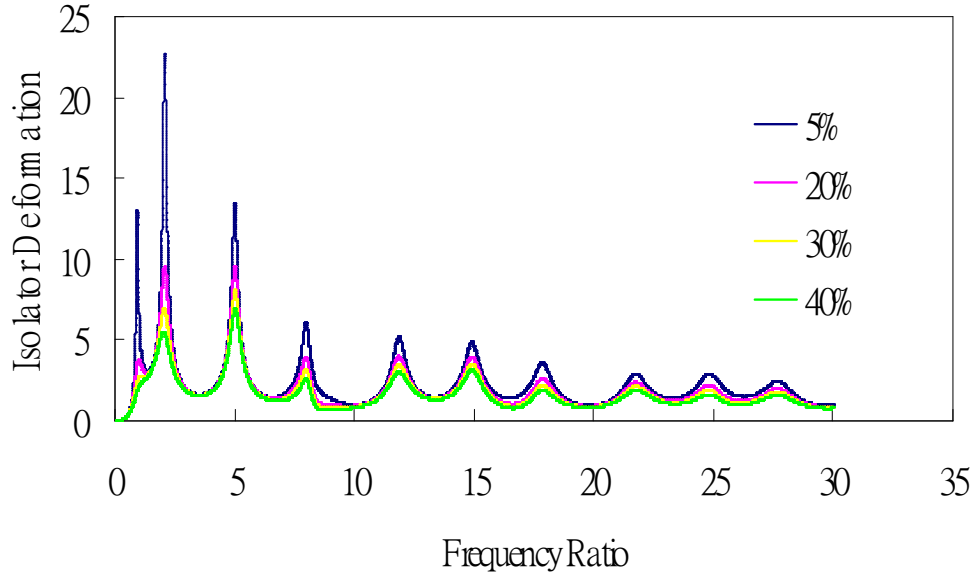

Figure 19. Isolator deformation for Case 2-2 under various damping ratio of isolator